

Measuring the plasma density of a ferroelectric plasma source in an expanding plasma

A. Dunaevsky and N. J. Fisch

Princeton Plasma Physics Laboratory, Princeton University, P.O. Box 451, Princeton, New Jersey 08536

(Received 19 September 2003; accepted 9 February 2004)

The initial density and electron temperature at the surface of a ferroelectric plasma source were deduced from floating probe measurements in an expanding plasma. The method exploits negative charging of the floating probe capacitance by fast flows before the expanding plasma reaches the probe. The temporal profiles of the plasma density can be obtained from the voltage traces of the discharge of the charged probe capacitance by the ion current from the expanding plasma. The temporal profiles of the plasma density, at two different distances from the surface of the ferroelectric plasma source, could be further fitted by using the density profiles for the expanding plasma. This gives the initial values of the plasma density and electron temperature at the surface. The method could be useful for any pulsed discharge, which is accompanied by considerable electromagnetic noise, if the initial plasma parameters might be deduced from measurements in expanding plasma. © 2004 American Institute of Physics. [DOI: 10.1063/1.1690860]

INTRODUCTION

Ferroelectric plasma sources (FPS) are attractive because of their ability to generate surface plasma on, in principle, unlimited area of the surface of ferroelectric ceramics covered by a patterned electrode. The principle of FPS operation is based on the ability of ferroelectric materials to buildup substantial polarization charge in response to a driving pulse application.^{1–3} The patterned structure of the front electrode induces a strong nonuniformity of the surface distribution of the polarization charge, which leads to substantial electric fields along the ceramic surface. At the edges of the patterned electrode, the electric field is sufficient for the field emission from triple junctions.⁴ Avalanching of field emission electrons along the ceramic surface causes the formation of plasma, which consists mostly of the materials of ferroelectric ceramics and the patterned electrode.⁵

Diagnosing the FPS plasma is usually complicated by practical difficulties. The intrusion of small-scale probes in the near-surface region of the discharge perturbs substantially the distribution of the surface charge and consequently the operation of FPS. Optical spectroscopy is the preferred diagnostic tool for FPS. Spectroscopic study of the FPS⁵ showed that the plasma has a density of about 10^{12} cm⁻³ and an electron temperature near 3 eV. However, spectroscopic measurements on submicrosecond time scales are complicated and require collision-radiative codes for the modeling of nonsteady-state plasmas.⁵ In the majority of experiments, plasma measurements were performed in expanding plasma by probes placed distantly from the FPS surface.^{6–9} Although placed distantly, the probes are exposed to strong broadband electromagnetic noise from the surface discharge. Consequently, measurements of the ion saturation branch of the ampere-volt characteristics of a biased probe, where the probe signal is usually very low, become uncertain on the noise background of hundreds of millivolts. Hence, only an estimation of the plasma density. Sheath instabilities could also lead to modulation of the probe signal. The suppression

of the high-frequency modulation of the probe signal by limiting the bandwidth of the probe circuit is not always possible, because the time scale of the processes to be described is close to the period of the noise oscillations. Fast plasma flows, which are formed at the initial stage of the surface discharge, also disturb the signal of a single probe. Because of these reasons, most of the probe measurements in previous studies of FPS were done by biased probes placed behind a grounded grid, which helped to suppress the noise.^{6–9} Measurements of the density of expanding plasma behind the grounded grid left some uncertainty in the original plasma density because of grid transparency, which is not easy to evaluate accurately. Consequently, reliable temporal profiles of the plasma density in the expanding FPS plasma were not obtained yet.

Floating probes are usually used in steady state plasmas for measuring the plasma potential. In nonstationary plasmas in presence of fast non-neutral flows, like the FPS plasma, floating probes not always can provide correct information about the plasma potential. Indeed, energetic plasma flows, which are formed at the beginning of FPS operation,¹⁰ charge the capacitance of the floating probe up to the potential of hundreds of volts. Even for minimized probe capacitance, the time constant of the probe circuit is much higher than the time scale of changing plasma parameters. The probe potential cannot follow the temporal changes of the plasma potential, which makes it impossible to determine the plasma potential.

However, observation of the discharge process of the floating probe capacitance was found to be useful for determination of temporal behavior of the plasma density. Indeed, the floating probe can be considered as a conductor in vacuum, precharged up to a high negative potential φ_0 by the energetic non-neutral plasma flows. The probe is connected to the ground by a very high resistance R and a small capacitance C . The time constant RC is much higher than the time scale of the process, so the discharge of the probe by the leak current through the resistance R can be neglected. When an

expanding quasineutral plasma reaches the probe, the ion flux from the plasma discharges the probe. The rate of increase of the probe potential $\varphi(t)$ is proportional to the total ion current $i(t)$ to the probe

$$\frac{d}{dt}\varphi(t) = \frac{i(t)}{C}. \quad (1)$$

In case of a high negative potential, neglecting the secondary electron emission from the probe, the current $i(t)$ is the ion saturation current¹¹

$$i_{is}(t) = j_{is}(t)S(t) = 0.52Zen_i(t)V_B S(t). \quad (2)$$

Here Ze is the ion charge, $n_i(t)$ is the ion density at the location of the probe, V_B is the Bohm velocity, and $S(t)$ is the surface area of the ion current collection. Based on previous results,^{5,6,10} the expanding bulk plasma of FPS can be assumed quasineutral, consisting mostly of singly charged ions, i.e., $n_i(t) \approx n_e(t) \approx n(t)$ and $Z=1$. By measuring the wave form of the conductor potential, $\varphi(t)$, one can obtain the plasma density $n(t)$, if the plasma electron temperature T_e and the surface of the current collection $S(t)$ can be evaluated. Notice that the initial negative potential φ_0 , which is acquired by the probe from the energetic flow with poor repeatable parameters, varies significantly from shot to shot. However, the deduced density profile $n(t)$ does not depend on the conditions of the probe charging but only on the discharge process. In general, the probe can be pre-charged to an arbitrary (but sufficiently high) negative potential from any external voltage source.

Surface discharge plasma of FPS is essentially multi-component, consisting of ions of the ferroelectric ceramics and the patterned front electrode.⁵ The Bohm criterion for multicomponent plasma was formulated by Riemann as¹²

$$\begin{aligned} 1 &\geq \sum_q \left(\frac{n_q}{n_e} \frac{kT_e}{A_q m_p v_q^2 - \gamma kT_q} \right) \approx \sum_q \left(\frac{n_q}{n_e} \frac{kT_e}{A_q m_p v_q^2} \right) \\ &= \sum_q \left(\frac{n_q}{n_e} \frac{C_q^2}{v_q^2} \right), \end{aligned} \quad (3)$$

where n_q , A_q , and v_q are the density, the atomic weight, and the velocity of q th ion specie, respectively, m_p is the proton mass, and

$$C_q = \sqrt{\frac{kT_e}{A_q m_p}} \quad (4)$$

is the ion sound velocity for q th ion specie. The inequality (3) can be satisfied if either each fraction has its own Bohm velocity, or all ions have the same velocity V_{Bm} . Hala *et al.*,¹³ assumed the same Bohm velocity for all species

$$V_{Bm} = \sqrt{\sum_q \frac{n_q}{n_e} C_q^2}. \quad (5)$$

This result was confirmed by the recent study of the sheath in two-component plasma, performed by Severn *et al.*¹⁴ Based on the similarity of experimental conditions, we assume here as well that all species in multicomponent FPS plasma have the same Bohm velocity in the form of Eq. (5).

The surface area $S(t)$ for a thick cylindrical probe with a radius r_0 and a length l is determined by the sheath thickness $h_s(t)$:

$$S(t) = 2\pi[r_0 + h_s(t)]l. \quad (6)$$

The thickness of a unipolar sheath in the space charge saturation for high negative probe potentials, when $V_B \ll \sqrt{2e\varphi/M_i}$, could be estimated as

$$h_s(t) \approx \lambda_D(t) \frac{\sqrt{2}}{3} \left[\frac{2\varphi(t)}{kT_e} \right]^{3/4}, \quad (7)$$

where $\lambda_D(t)$ is the Debye length:

$$\lambda_D(t) = \sqrt{\frac{kT_e}{4\pi n(t)e^2}}. \quad (8)$$

Equation (7) represents the solution of Poisson's equation with zero initial velocities of ions entering the collisionless sheath, which has a step-like electron density at the sheath boundary. However, Riemann and Tsengin¹⁵ developed a model of a unipolar sheath with appropriate initial conditions, which takes into account effects of presheath and influence of ion collisions in the thick unipolar sheath. According to Riemann and Tsengin, the sheath thickness can be represented more precisely as¹⁵

$$h_s(t) \left[1 + \frac{12\pi h_s(t)}{125\lambda} \right]^{1/4} = \lambda_D(t) \left[\sqrt{2Y} \left(\frac{Y}{3} + 2 \right) - 1.8197 \right], \quad (9)$$

where λ is the ion mean free path and

$$Y = \sqrt{1 + 2 \frac{e\varphi(t)}{kT_e}} - 2. \quad (10)$$

We found that the difference in the plasma density, derived with the use of Eq. (7) or Eq. (9), can reach 30%. Therefore, more precise model by Riemann and Tsengin was applied for the data processing.

Solving together the Eqs. (1), (2), (5), (6), and (9), and using the measured waveform of the probe potential $\varphi(t)$, we can deduce the slope of the density $n(t)$ of the bulk plasma expanding outward the front surface of the FPS. The electron temperature T_e in the expanding plasma is assumed to be about 3 eV from spectroscopic measurements.⁵ The same value of T_e was obtained in earlier measurements by double floating probes.⁶ Notice that a multi-Maxwellian electron temperature was observed in experiments with multi-component plasma.¹⁴ However, there is still no thorough data for the electron temperature of FPS plasma. Thus, here we assume the value of $T_e = 3$ eV as a mean electron temperature of the system. We also assume T_e independent on time and the driving pulse amplitude, which was indicated in Ref. 5.

EXPERIMENTAL SETUP

Our experimental setup, presented schematically in Fig. 1, is similar to other setups for study of FPS.¹⁻¹⁰ The ferroelectric plasma source consists of a ferroelectric disc made of $\text{Pb}(\text{Zr}_x\text{Ti}_{1-x})\text{O}_3$ (PZT) ceramics APC-850 ($\epsilon = 1750$). The disk has a diameter of 38 mm and a thickness of 2 mm. The

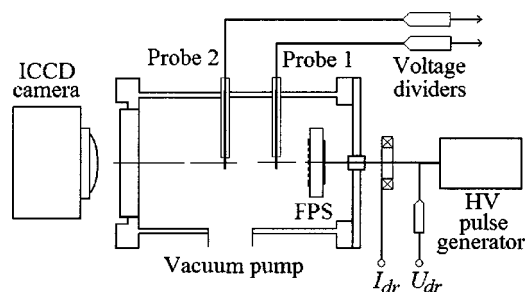


FIG. 1. Experimental setup.

grounded front electrode has a pattern in form of 1 mm strips interconnected by an outer copper ring with a diameter of 20 mm, which was glued to a brass flange by a conducting epoxy. A driving pulse was applied to a rear disk electrode made of copper. A negative driving pulse with a duration of ~ 500 ns full width at half maximum was supplied by a Blumlein pulse generator, matched by a 50Ω resistor. The amplitude of the driving pulse was varied from 3 to 6 kV. The repetition rate of the driving pulses was 1 Hz. The driving voltage was measured by LeCroy voltage divider; the current supplied to the FPS was measured by Pearson Rogovski Coil. Signal wave forms were recorded by Tektronix DSO 5054 digital oscilloscope.

Cylindrical probes were placed at 5.5 and 14 mm from the front surface of the FPS. In order to decrease the effect of screening of the second probe by the first one, the second probe was mounted with azimuthal displacement of 90° with respect to the first probe. The probes were made of tungsten wire with a diameter of 1.5 mm. The wire was inserted into a tube made of alumina ceramics, which in its turn was placed inside a stainless steel shielding tube. This coaxial structure was connected directly to an SMA connector. Such a design provides a wide bandwidth of the probe. The point of connection to the SMA connector was sealed vacuum-tightly by Saurisen alumina glue. The probes were immersed in the vacuum chamber through Wilson seals. The vacuum chamber had a diameter of 10 cm, which was sufficient for applicability of the model of free plasma expansion in vacuum for the first $2.5\text{--}3 \mu\text{s}$. Indeed, plasma flow with the expansion velocity of about $2 \text{ cm}/\mu\text{s}$ will reach the walls in $2.5 \mu\text{s}$. Later on, the measured density profile would be disturbed because the presence of walls.

The signals from the probes were measured by Tektronix 5052 voltage dividers and recorded by the Tektronix DSO 5054 digital oscilloscope simultaneously with the driving voltage and the driving current. The voltage dividers have an input resistance of $R = 10 \text{ M}\Omega$ and provide a bandwidth of 100 MHz. The total capacitance of the assembly (probe and voltage divider) was determined from the following procedure. After mounting of the probes at their actual position in the vacuum chamber, the probe tip was connected to the ground by a high precision resistor of $R_t = 9.09 \text{ k}\Omega$ and to a dc power supply by a switch. The probes were charged from the power supply up to 60 V, and the wave forms of the discharge, after disconnecting the power supply, were recorded. The probe capacitance C was deduced from the time constant of the discharge of C via $R_t \ll R$. The capacitances

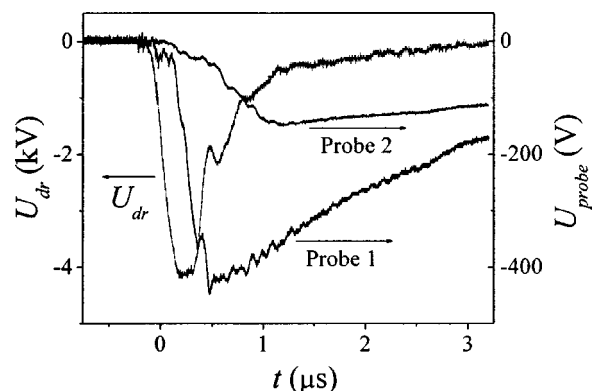


FIG. 2. Typical potentials observed from a pair of floating probes placed at distances of 5.5 mm (probe 1) and 14 mm (probe 2) from the front surface of the FPS.

of the probe assemblies were $C_1 = 21 \text{ pF}$ and $C_2 = 28 \text{ pF}$ for the first and the second probes, respectively.

Operation of the FPS with probes was observed by Andor I-Star[®] ICCD camera. It allowed us to make sure in the absence of the plasma formation at the probe tips. Plasma formation on the probe tip turns the probe from nonemissive floating mode to emissive floating mode. This effect was used for measurement of the potential distribution between the FPS surface and the grounded output grid in the case of generation of high-frequency modulated electron beam.¹⁶ The possible reason of this effect is the high potential of the fast flows, which are formed at the initial stage of the FPS operation.¹⁰ In earlier works, we observed the plasma formation on the tips of biased probes, which were close to the ground potential. In the present study, we used this effect for cleaning the probe tips before the measurements.

The full setup was pumped down to $\sim 8 \times 10^{-7}$ Torr by an oil-free pumping station. Deep oil-free vacuum is preferable for the reduction of light ion components in the plasma. Indeed, a spectroscopic study indicated that, in clean conditions, FPS plasma consists mostly from heavy elements of the ceramic compound.⁵ For our $\text{Pb}(\text{Zr}_x\text{Ti}_{1-x})\text{O}_3$ ceramics, one could expect the presence of Pb ($A = 207$), Zr ($A = 91$), Ti ($A = 48$), and O ($A = 16$). The predominance of these elements during the FPS operation was confirmed by measurements of the residual gases during the FPS operation. These measurements were performed by the use of RSA-300 residual gas analyzer produced by Stanford Research Systems. We found that, after 10–15 min of FPS operation, the concentration of light elements like carbon and hydrogen was insignificant in comparison with lead, zirconium, titanium, and oxygen. However, the amplitude of oxygen spectral lines in Ref. 5 was found relatively small in spite of optically thin plasma. Comparatively small fraction of oxygen ions could be explained by the low electron temperature and the high ionization potential of oxygen.

EXPERIMENTAL RESULTS

Typical signals from both probes are shown in Fig. 2 together with the driving pulse wave form. The driving pulse starts at $t = -100$ ns and has a rise time of $\tau_f \approx 250$ ns. The

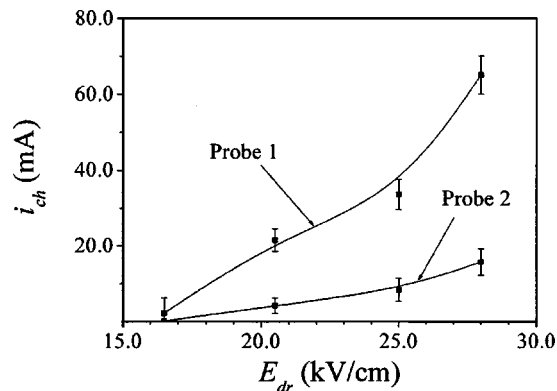


FIG. 3. Negative charging current vs the driving electric field amplitude.

charging of the probes begun at $t \approx 100$ ns, which coincides well with the time of intense plasma formation on the FPS surface, as observed by ICCD camera. The charging rate is almost constant for both probes, corresponding to constant charging current. The current of the probe charging depends on the driving voltage amplitude, as illustrated by Fig. 3.

The process of the initial charging of the probes is not understood completely yet. The charging of the second probe lasts as long as $1 \mu\text{s}$ with almost constant charging rate. The probes are not in emissive mode and their potential cannot follow the space potential. Thus, the probes could be charged either by a fast flow or by a capacitive pickup. However, the capacitive pickup from the driving pulse, measured without plasma formation, was found to be negligibly small. Therefore, we believe that the fast non-neutral flows, which are formed during the FPS plasma formation, could contribute to the probe charging.¹⁰ Maximal potential $\varphi_{0 \text{ max}}$ of the probe charging is limited by the maximal energy of electrons in the flows. This maximal energy reaches several kilo-electron-volts,¹⁷ which coincides well with the observed probe potentials.

The process of the probe charging is interrupted when the front of the quasineutral bulk plasma reaches the probes. The probe capacitance is then discharged by the ion current. This point in time is easily recognizable from the probe signals (see Fig. 2). The variation of the probe potential, $d\varphi(t)/dt$, is easily found, so that the ion density $n_i(t)$ of the expanding bulk plasma can then be obtained from Eqs. (1), (2), (5), (6), and (9). Figure 4 represents $n_i(t)$ measured by the first probe (at the distance of 0.55 cm from the FPS surface) for the driving electric field amplitudes of 16.5, 20, and 25 kV/cm. The expanding bulk plasma is likely quasineutral, so that the measured ion density $n_i(t)$ is equal to the plasma density $n(t)$. Note that the plasma is more uniform at low driving pulse amplitudes. At higher amplitudes, the density is perturbed by oscillations which correlate with the driving current oscillations. At the driving electric field higher than 25–28 kV/cm, the growth of the plasma density saturates at the level of about $2 \times 10^{12} \text{ cm}^{-3}$.

At $t \approx 2.75 \mu\text{s}$, a fast ion flow was observed. The peck of the ion current appears almost simultaneously on both probes (see Fig. 4). From the time delay between peck appearance, we found the velocity of this fast flow of about 10^8 cm/s .

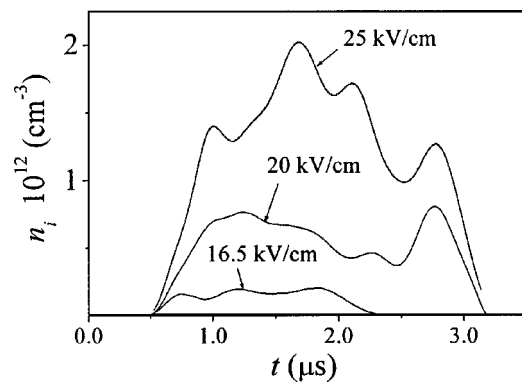


FIG. 4. Ion density of the expanding bulk plasma at 5.5 mm from the front surface of the FPS for driving electric field amplitudes of 16.5, 20, and 25 kV/cm.

The formation of fast flows during the FPS operation was described in Ref. 10.

From the measured plasma density, we can calculate the electron saturation current density

$$j_{\text{es}} = j_{\text{is}} \sqrt{\frac{M_i}{m_e}}. \quad (11)$$

Here m_e and M_i are the electron and ion mass, respectively. The value of j_{es} should be compared with the current density measured earlier in a planar electron diode with BaTiO₃ ferroelectric cathode.⁶ The electron saturation current density, calculated for the present experiments with PZT ceramics, and the electron current density, obtained in Ref. 6 with BaTiO₃ ceramics, are shown in Fig. 5. For the both ferroelectric materials, the electron saturation current density is in the same order of magnitude and behaves linearly with the driving electric field. This can be considered as an indirect confirmation of the validity of the present density measurements in the expanding plasma. The difference in the absolute values and in the slopes of curves may be caused by differences in the experimental conditions.

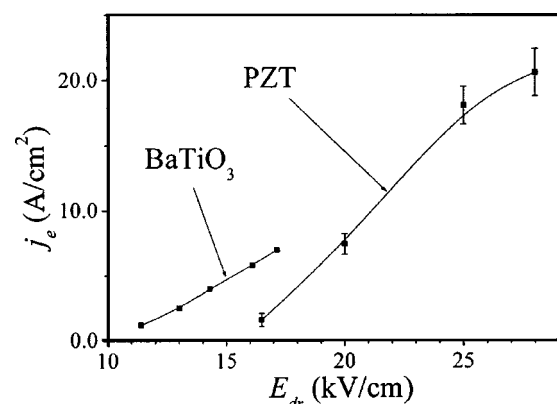


FIG. 5. Electron saturation current density measured in an electron diode with BaTiO₃ ferroelectric cathode (accepted from Ref. 6) and calculated electron saturation current density for measured ion density for PZT ferroelectric plasma source (present measurements).

DISCUSSION

The temporal profiles of the plasma density that we deduce, together with a theoretical model of the plasma expansion into vacuum, can be used to deduce the initial plasma density $n(x=0,t=0) \equiv n_0$ and the temperature $T_e(x=0,t=0) \equiv T_{e0}$ in the stems of surface discharges at the FPS surface. The problem of plasma expansion into vacuum has been treated by the pioneering works of Gurevich *et al.*¹⁸ The isothermal model by Gurevich *et al.* was formulated for a uniform infinite plasma occupied a half-space $x < 0$. This approach implies infinite mass and energy in the system, making it inapplicable for the case of expansion of finite plasma bunches. Recently, driven by growing interest to the ion acceleration in the expanding plasma formed by ultrashort laser pulses, self-similar analytical solutions of the kinetic equations for adiabatic collisionless expansion of finite plasma bunches were obtained for one-dimensional (1D)^{19,20} and three-dimensional (3D)^{21,22} problems with various initial conditions. These solutions could be valid also for pulsed surface discharges, where the time of the plasma formation is also shorter than the time scale of plasma expansion. Here, we apply a 1D model proposed by Kovalev *et al.*²⁰ in order to deduce of the initial plasma density and electron temperature at the FPS surface from the measured density profiles.

According to the applied model, the ion density profile $n(x,t)$ can be approximately expressed as²⁰

$$n(x,t) \approx \frac{n_0}{\sqrt{1 + \Omega^2 t^2}} \exp\left(-\frac{U^2}{2C_s^2}\right), \quad (12)$$

where n_0 is the plasma density at $x=0$ and $t=0$. The frequency Ω is specified by the ratio of the ion sound velocity to the initial scale of inhomogeneity of the plasma density, which is about of the initial Debye length λ_{D0} :

$$\Omega^2 \sim 2 \frac{C_s^2}{\lambda_{D0}^2}. \quad (13)$$

In Eqs. (11) and (12), we used the Bohm velocity for multi-component plasma from Eq. (5). The characteristic velocity U is given as

$$U(x,t) = \frac{\Omega x}{\sqrt{1 + \Omega^2 t^2}}. \quad (14)$$

This solution implies initial Maxwellian distribution function for electrons with $T_{e0} \gg T_{i0}$. This assumption might be valid for the case of surface discharges, where the time scale of the plasma formation is sufficient for the equilibration of initially dense plasma.

Using T_{e0} and n_0 as parameters, it is possible to find a pair of density profiles, $n(x_1,t)$ and $n(x_2,t)$, which will fit the measured densities at two probe locations, $x_1 = 5.5$ mm and $x_2 = 14$ mm. Typical result of such an attempt is shown in Fig. 6 for $E_{dr} = 20$ kV/cm. The best fit was obtained with $n_0 = 6 \times 10^{16} \text{ cm}^{-3}$ and $T_{e0} = 16$ eV. Note the coincidence between measured and calculated profiles for the location of the first probe. The time delay between two profiles, which characterize the velocity of the plasma expansion, also coin-

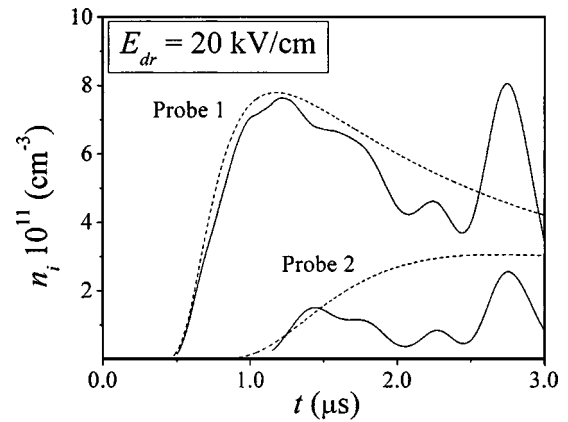


FIG. 6. Ion density of the expanding bulk plasma, measured by floating probes placed at distances of 5.5 mm (probe 1) and 14 mm (probe 2) from the front surface of the FPS, in comparing with ion density of expanding plasma with an initial density of $6 \times 10^{16} \text{ cm}^{-3}$ and an initial temperature of 16 eV, calculated in accordance with the model of Kovalev *et al.* (see Ref. 21).

cides well with the measurements. The best fit for the driving electric field of 25 kV/cm was obtained with $n_0 = 4 \times 10^{17} \text{ cm}^{-3}$ and $T_{e0} = 18$ eV. For $E_{dr} < 18$ kV/cm, the signal from the second probe was too small to find an appropriate fit. At $E_{dr} > 25$ kV/cm, the initial plasma density was found about the same as for 25 kV/cm, while the initial electron temperature reached 20–22 eV. The calculated profiles for the location of the second probe, however, showed usually higher density and longer plasma pulse than it was observed experimentally.

Excluding the fast plasma flow at $t \approx 2.75 \mu\text{s}$, the gradient of the plasma density was found monotonically decreasing in time. The gradient of the plasma density was determined as a difference in the plasma density measured by two probes $\delta n(t) = n(x_1,t) - n(x_2,t)$, divided by the distance between probes $\delta x = x_2 - x_1$. The measured and calculated gradients for two driving pulse amplitudes are shown in Fig. 7. There also appears to be agreement between the shapes of measured and calculated profiles. This agreement, together with the agreement in the density profiles and the expansion velocity, validates in general the applicability of the model of plasma expansion for deducing the initial plasma density and electron temperature of the FPS plasma. The deduced values

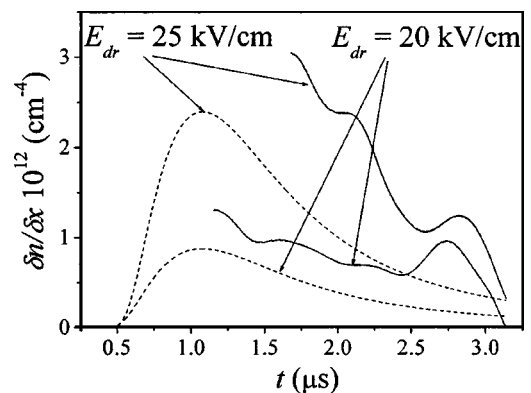


FIG. 7. Comparison of measured and calculated gradients of the expanding plasma density for different driving electric field amplitudes.

of the initial plasma density in the stem of the surface discharge also agree in order of magnitude with the typical plasma density in the high-pressure arc,²³ which is suggested as a final stage of the surface flashover:²⁴ $n \sim 10^{15} - 10^{17} \text{ cm}^{-3}$.

However, the difference in absolute values of density gradients, as well as the difference in the shape of density profile at the location of the second probe, indicate a discrepancy between applied model and the measurements. This discrepancy could be caused by several possible reasons. First, we applied here the 1D model, which is valid if the distances to the probes $x_{1,2}$ are much less than the diameter of the plasma source, d , $x_{1,2} \ll d$. A recently developed 3D model of the expansion of plasma from a point-like source,²² however, is relevant only if $x_{1,2} \gg d$. In general, a fully 3D model is required for the case $x_{1,2} \sim d$, which is realized in our experimental conditions. The 1D model predicts longer plasma tail and slower decrease of the density at the location of the probe 2, where $x_2 \sim d/2$ (see Fig. 6). However, the agreement with the measurements is much better for the probe 1, where $x_1 \sim d/4$ and the 1D model is more relevant.

Second, we simplified the problem of the expansion of multicomponent plasma by application of the model formulation for monocomponent plasma expansion but with Bohm velocity for multicomponent plasma. This simplification is justified for the present experiments, because the proportion in the ion mixture was only estimated. Better knowledge about the proportion in the ion species mixture, and the use of the model of expansion of multicomponent plasma,²⁰ should result in higher precision of the deduced n_0 and T_{e0} .

Third, the applied model of plasma expansion does not take into account processes of ionization and recombination. This assumption is valid for laser plasma, where the time scales of ionization and recombination are not comparable with the time slot in calculations. In the case of FPS and other surface discharges, the process of plasma formation may last up to 50–100 ns, which is only 5–10 times less than the time scale of our measurements. The longer process of plasma formation could lead to overestimation of the initial plasma density. More precise results can be obtained with the addition of ionization and recombination terms to the Vlasov equation in the model of plasma expansion. In such form, however, the Vlasov equation would unlikely be integrated analytically, and the deducing of initial plasma density and temperature will require much more complicated numerical procedure.

SUMMARY

We describe here a method of deducing the plasma density in the expanding plasma of FPS. The effect of negative charging of the floating probe capacitance by fast flows is employed. Observing the discharge of charged probe capacitance by the ion current from the expanding bulk plasma of the FPS source, temporal profiles of the plasma density can be obtained. The advantage of the described approach is in voltage measurements in the order of hundreds of volts, which should be several orders of magnitude higher than the noise amplitude.

The temporal profiles of the plasma density at two different distances from the FPS surface can then be fitted by analytical profiles for the expanding plasma, from which we can deduce the initial values of the plasma density and electron temperature at the surface of the FPS. For PZT-based FPS, the initial plasma density is in the range of $n_0 = (0.4 - 4) \times 10^{17} \text{ cm}^{-3}$ and the initial electron temperature is $T_{e0} = 16 - 20 \text{ eV}$ for the driving electric fields of 16–30 kV/cm. This result, however, was obtained in assumption of momentary plasma formation with the use of the 1D model of plasma expansion, which could cause uncertainty in deduced values of n_0 and T_{e0} . A more accurate model of plasma formation and expansion, as well as better knowledge about proportions in the ion species mixture, could make the deduction more precise. Nevertheless, the method of density measurements in the expanding plasma and the deduction of the initial values of plasma density and temperature may be useful also for other kinds of short-time discharges accompanied by considerable electromagnetic noise.

ACKNOWLEDGMENTS

The authors gratefully acknowledge Dr. Y. Raitsev, Dr. I. Kaganovich, and Dr. E. Startsev for very fruitful discussions. They also thank R. Yager and G. d'Amico for technical support. This work was supported by the New Jersey Commission of Science and Technology, and by the DOE under Contract No. DE-AC02-76-CH03073.

¹G. Rosenman, D. Shur, Kh. Garb, R. Cohen, and Ya. E. Krasik, *J. Appl. Phys.* **82**, 772 (1997).

²G. Rosenman, D. Shur, Ya. E. Krasik, and A. Dunaevsky, *J. Appl. Phys.* **88**, 6109 (2000).

³I. Boscolo and S. Cialdi, *J. Appl. Phys.* **91**, 6125 (2002).

⁴V. F. Puchkarev and G. A. Mesyats, *J. Appl. Phys.* **78**, 5633 (1995).

⁵A. Dunaevsky, K. Chirko, Ya. E. Krasik, J. Felsteiner, and V. Bershtam, *J. Appl. Phys.* **90**, 4108 (2001).

⁶A. Dunaevsky, Ya. E. Krasik, J. Felsteiner, and S. Dorfman, *J. Appl. Phys.* **85**, 8464 (1999).

⁷A. Dunaevsky, Ya. E. Krasik, J. Felsteiner, and A. Sternlieb, *J. Appl. Phys.* **90**, 3689 (2001).

⁸A. Krokmal, J. Z. Gleizer, Ya. E. Krasik, and J. Felsteiner, *J. Appl. Phys. Lett.* **81**, 4341 (2002).

⁹A. Dunaevsky, Y. Raitsev, and N. J. Fisch, *J. Appl. Phys.* **93**, 3481 (2003).

¹⁰A. Dunaevsky, Ya. E. Krasik, J. Felsteiner, and A. Sternlieb, *J. Appl. Phys.* **91**, 975 (2002).

¹¹Yu. P. Raizer, *Gas Discharge Physics* (Springer, Berlin, 1997), Chap. 6, p. 115.

¹²K. U. Riemann, *IEEE Trans. Plasma Sci.* **23**, 709 (1995).

¹³A. M. Hala and N. Hershkovitz, *Rev. Sci. Instrum.* **72**, 2279 (2001).

¹⁴G. D. Severn, X. Wang, E. Ko, and N. Hershkovitz, *Phys. Rev. Lett.* **90**, 145001 (2003).

¹⁵K. U. Riemann and L. Tsendin, *J. Appl. Phys.* **90**, 5487 (2001).

¹⁶A. Dunaevsky, Ya. E. Krasik, J. Felsteiner, and A. Rosenberg, *J. Appl. Phys.* **86**, 4107 (1999).

¹⁷A. Dunaevsky, Ya. E. Krasik, J. Felsteiner, and A. Krokmal, *J. Appl. Phys.* **87**, 3270 (2000).

¹⁸A. V. Gurevich, L. V. Pariskaya, and L. P. Pitaevskii, *Sov. Phys. JETP* **22**, 449 (1966).

¹⁹A. V. Baitin and K. M. Kuzanyan, *J. Plasma Phys.* **59**, 83 (1998).

²⁰V. S. Kovalev, V. Yu. Bychenkov, and V. T. Tichonchuk, *Sov. Phys. JETP* **95**, 226 (2002).

²¹D. S. Dorozhkina and V. S. Semenov, *Phys. Rev. Lett.* **81**, 2691 (1998).

²²V. F. Kovalev and V. Yu. Bychenkov, *Phys. Rev. Lett.* **90**, 185004 (2003).

²³Yu. P. Raizer, *Gas Discharge Physics* (Springer, Berlin, 1997), Chap. 10, p. 273.

²⁴H. C. Miller, *IEEE Trans. Plasma Sci.* **24**, 765 (1989).